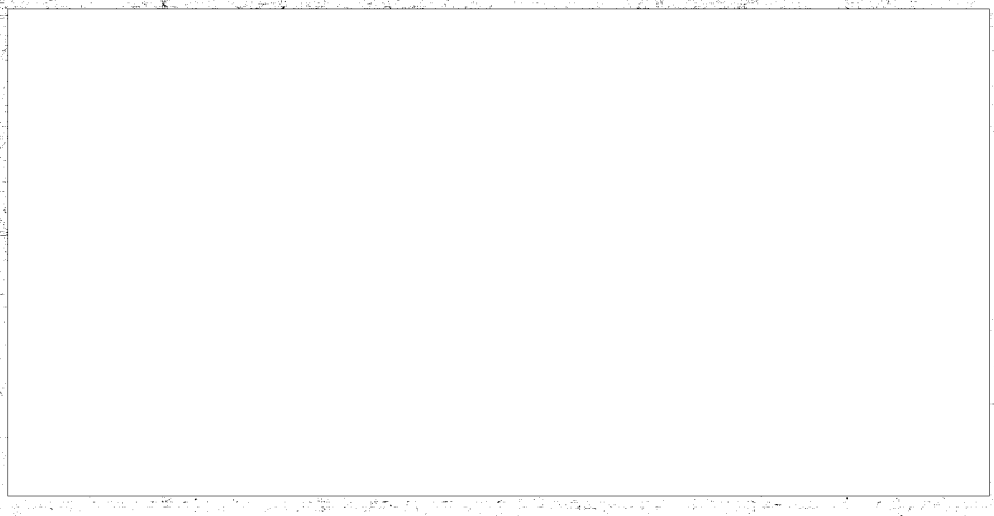

THE BALLISTIC DEMAGNETISATION FACTOR OF CYLINDRICAL BARS

K. Warmuth

Archiv für Elecktrotechnik, 32 (1939) 747 - 763

(From German)

25X1

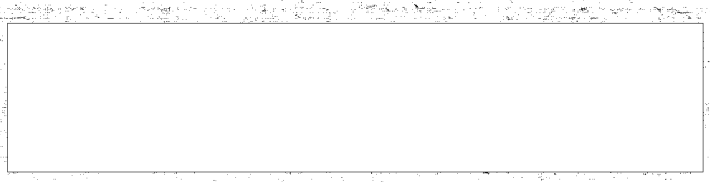

August, 1955

THE BALLISTIC DEMAGNETISATION FACTOR OF CYLINDRICAL BARS

K. Warmuth

Archiv für Elektrotechnik, 32 (1939) 747-763
(From German)

SUMMARY

The ballistic demagnetisation factors of cylindrical bars are determined for dimension ratios $p < 10$ down to $p = 0$ and for any susceptibilities $0 < \kappa < \infty$. Furthermore, the importance of the ballistic demagnetisation factor for the evaluation of magnetic measurements is discussed in detail.

I. STATEMENT OF THE PROBLEM

In an earlier paper by the author [1]*, it was shown that by using the demagnetisation factors of ellipsoids N_{ell} it is possible, both for the limit case of infinitely high susceptibility** $\kappa = \infty$ and for the susceptibility $\kappa = 0$, to derive simple expressions for the ballistic demagnetisation factor in the range $p < 10$ (p = ratio of length to diameter of the cylindrical bar). The solution was there reduced to the determination of approximation straight lines by the method of least squares.

In the following a method is given which leads in a different way, but likewise with the use of the demagnetisation factor of ellipsoids, to simple derivations for the two limit cases of the ballistic demagnetisation factor in the range $0 \leqq p \leqq 100$. It will also be shown that physically understandable results are obtained with the new formulae, and in addition sufficient agreement with experiment is obtained for ratios of practical interest.

Furthermore, for the range $0 \leqq \kappa < \infty$ and $p < 10$, which previously has not been considered either theoretically or experimentally, an attempt is made to determine the ballistic demagnetisation factor both by the method of approximation straight lines and graphically.

Finally, the paper deals with a critical consideration of the importance of the ballistic demagnetisation factor for the evaluation of magnetic measurements.

II. GENERAL PRINCIPLES

The premises previously made will also be retained for the present investigations, i.e. the discussions are based in the first place on the fact that for $p = 0$, the demagnetisation factor is equal to 4π, i.e.

$$[N_{ell}]_{p=0} = [N_{0 \leqq \kappa \leqq \infty}]_{p=0} = 4\pi . \qquad \ldots\ldots (1)$$

---

* For references, see end.

** $\kappa = \frac{\mu - 1}{4\pi}$ where μ is the permeability of material. This equation is a numerical equation. According to the new rules of the Archiv f. Elektrotechn., this expression as dimension equation would be

$$\kappa = \frac{\mu - \mu_0}{4\pi}$$

where μ_0 is the permeability of vacuum.

Secondly, the mathematical assumption is made that the demagnetisation factor $N_{0 < \kappa < \infty}$ with decreasing dimension ratios D approaches the limit value 4π steadily and monotonically, as is also the case, furthermore, with the demagnetisation factor of the ellipsoid.

We shall now give the formulae which are necessary for the subsequent discussions. For the susceptibility $\kappa = 0$, E. Dussler [2] has developed the relationship

$$N_{\kappa = 0} = \frac{2\pi}{p^2}, \quad p \geq 10 \qquad \ldots\ldots (2)$$

The case of infinitely high susceptibility $\kappa = \infty$ may be reproduced by the following interpolation formula of the author [3]:

$$N_{\kappa = \infty} = 0.667 \cdot p^{0.05} \cdot N_{ell}, \quad 10 \leq p \leq 500 \qquad \ldots\ldots (3)$$

The formula of Stäblein and Schlechtweg [4] gives the ballistic demagnetisation factor of cylindrical bars for dimension ratios $D \geq 10$ and susceptibilities $0 \leq \kappa \leq \infty$ [5]*:

$$N = \frac{2\pi}{p^2}\left[1 - 6\,t^2 + 30\,t^4 - 1.40\,t^6 - \frac{c_1}{c_0}\left[-2\ln t - 3 - \right.\right.$$
$$\left.\left. - 4\,t^2 + 51\,t^4 - \frac{880}{3}\,t^6\right]\right] \qquad \ldots\ldots (4)$$

where

$$t = \frac{1}{2p} \text{ and } \frac{c_1}{c_0} = f(p,\kappa) \qquad \ldots\ldots (5)$$

The demagnetisation factors of ellipsoids were determined from the two well-known expressions [6]

$$N_{ell} = \frac{4\pi}{p^2 - 1}\left[\frac{p}{\sqrt{p^2 - 1}} \ln\left(p + \sqrt{p^2 - 1}\right) - 1\right]; \quad p > 1 \qquad \ldots\ldots (6)$$

and

$$N_{ell} = \frac{4\pi}{1 - p^2}\left[1 - \frac{p}{\sqrt{1 - p^2}} \cos^{-1} p\right]; \quad p < 1 \qquad \ldots\ldots (7)$$

III. THE BALLISTIC DEMAGNETISATION FACTOR OF CYLINDRICAL BARS FOR DIMENSION RATIOS $p \leq 10$ AND SUSCEPTIBILITIES $0 \leq \kappa \leq \infty$

1. $N_{\kappa = 0}$ for $0 \leq p \leq 100$.

For a series of dimension ratios D between $p = 10$ and $p = 100$ we form the quotients $N_{ell}/N_{\kappa = 0}$ (see Table 1)**, plot this ratio linearly against p (Figure 1, curve 1) and extend the curve passing through these points to the point $[p = 0,\ N_{ell}/N_{\kappa = 0} = 1]$. It is now found that a function of the form

$$y = a \ln(1 + bx) + 1 \qquad \ldots\ldots (8)$$

reproduces this form of curve very well, if the values

$$a = 2.28 \text{ and } b = 0.284 \qquad \ldots\ldots (9)$$

are substituted for the constants a and b. We thus obtain

$$\frac{N_{ell}}{N_{\kappa = 0}} = 2.28 \ln(1 + 0.284\,p) + 1; \quad 0 \leq p \leq 100 \qquad \ldots\ldots (10)$$

---

* The deviation of the $N_{\kappa = \infty}$ = values calculated according to equation (3) from the values according to equation (4) is less than 3% as a mean in the D-range given.

** For Tables, see end.

The deviation of the individual values $N_{ell}/N_{K=0}$ calculated according to equation (10) from the quotients calculated from equations (2) and (6) is on the average less than 1% as follows from Table 1 for $p = 10$ to $p = 100$. Equation (10) now affords us the possibility of determining the magnitude $N_{ell}/N_{K=0}$ between $p = 0$ and $p = 10$ and hence also the demagnetisation factor N in this range.

For $N_{K=0}$ we have from equation (10):

$$N_{K=0} = \frac{N_{ell}}{2.28 \ln (1 + 0.284\, p) + 1}; \quad 0 \leqq p \leqq 100 \qquad \ldots\ldots (11)$$

The curves 2 and 3 in Figure 1 show the variation of the function $N_{ell}/N_{K=0} = f(p)$ for $0 \leqq p \leqq 10$ and $0 \leqq p \leqq 1$. Table 2 also gives for the same ranges the demagnetisation factors $N_{K=0}$ and $[N/4\pi]_{K=0}$ calculated according to equation (11).

2. $N_{K=\infty}$ for $0 \leqq p \leqq 100$.

Similarly, the demagnetisation factor $N_{K=\infty}$ in the limits $0 \leqq p \leqq 100$ can be determined from the quotient $N_{K=\infty}/N_{K=0}$.

If for $0 \leqq p \leqq 100$ the magnitude $N_{K=\infty}/N_{K=0}$ (see Table 3) is plotted linearly against the dimension ratio p (Figure 2, curve 1), this curve also can be represented by a function of the form (8) with suitable choice of the constants a and b. In this case, the magnitudes a and b have the values

$$a = 2.35 \text{ and } b = 0.137. \qquad \ldots\ldots (12)$$

For $N_{K=\infty}/N_{K=0}$ we then have from (8) and (12)

$$\frac{N_{K=\infty}}{N_{K=0}} = 2.35 \ln (1 + 0.137\, p) + 1 \qquad \ldots\ldots (13)$$

and hence

$$N_{K=\infty} = N_{K=0} [2.35 \ln (1 + 0.137\, p)] + 1; \quad 0 \leqq p \leqq 100. \qquad (14)$$

By transformation in conjunction with equation (11) we finally have

$$N_{K=\infty} = N_{ell} \frac{2.35 \ln (1 + 0.137\, p) + 1}{2.28 \ln (1 + 0.284\, p) + 1}; \quad 0 \leqq p \leqq 100 \qquad \ldots\ldots (15)$$

As will be seen from Table 3, the mean deviations of the values $N_{K=\infty}/N_{K=0}$ calculated according to (13) from the values calculated by division of $N_{K=\infty}$ and $N_{K=0}$ according to equations (2) and (3) are again less than 1% in the range $10 \leqq p \leqq 100$. Table 4 gives the demagnetisation factors $N_{K=\infty}$ and $[N/4\pi]_{K=\infty}$ calculated from equation (15) for $1 \leqq p \leqq 10$ and $0.1 \leqq p \leqq 1$. Curves 2 and 3 in Figure 2, similar to Figure 1, represent the variation of the function $N_{K=\infty}/N_{K=0} = f(p)$ for dimension ratios $p < 10$ and $p < 1$.

3. $N_{K=1}$ for $0 \leqq p \leqq 100$.

In addition to the limit cases $N_{K=0}$ and $N_{K=\infty}$ already mentioned, a simple derivation of the demagnetisation factor in the limits $0 \leqq p \leqq 100$ based on the principle of the approximation method is also possible for the case of the susceptibility $\kappa = 1$.

If, for $10 \leqq p \leqq 100$ we form the quotient $N_{K=\infty}/N_{K=1}$ by division of the $N_{K=\infty}$ values calculated from equation (3) and the $N_{K=1}$ values (cf. Table 5) determined from equation (4) or graphically and plot this expression linearly against p (Figure 3, curve 1), it is then possible by the method of least squares to draw a line, from which the points (.) do not deviate by more than 2% as a mean.

If the straight line is extended beyond $p = 10$, we see that the point $[p = 0; N_{K=\infty}/N_{K=1} = 1]$ also lies on this straight line. The quotient $N_{K=\infty}/N_{K=1}$ in the range $0 \leqq p \leqq 100$ can thus be represented by the following expression*:

$$\frac{N_{K=\infty}}{N_{K=1}} = 0.0485\, p + 1 . \qquad \ldots\ldots (16)$$

Substituting the value of $N_{K=\infty}$ from equation (15), we find the following expression for $N_{K=1}$

$$N_{K=1} = N_{ell} \frac{1 + 2.35 \ln (1 + 0.137\, p)}{[2.28 \ln (1 + 0.284\, p) + 1][0.0485\, p + 1]}; \quad 0 \leqq p \leqq 100. \qquad (17)$$

Curve 2 in Figure 3 reproduces on an enlarged scale the form of equation (16) in the range $0 \leqq p \leqq 10$. Table 6 shows the demagnetisation factors calculated by means of equation (17) for a series of p values between $p = 0$ and $p = 10$.

4. $N_{1 < \kappa \leqq 10}$ for $0 \leqq p \leqq 10$.

For determining the ballistic demagnetisation factor $N_{1 < \kappa \leqq 10}$ in the range $p < 10$ it was first of all necessary to calculate or determine graphically a number of N values for susceptibilities between $\kappa = 1$ and $\kappa = 10$ and dimension ratios $p > 10$ according to expression (4). Table 7 gives the demagnetisation factors for five different p and κ values, as well as the quotients $N_{K=\infty}/N_K$ formed with $N_{K=\infty}$ (cf. Table 3). If these quotients - for dimension ratios $10 < p < 50$ - are plotted linearly as a function of p, we obtain the family of curves shown in Figure 4. We now ask how do these curves run in the range $p < 10$. In accordance with the expression (1) established at the commencement, the magnitudes $N_{K=\infty}/N_K$ for $p \to 0$ must approach unit value. We can, therefore, prolong the curves of constant susceptibility κ beyond the point $p = 10$ to $p = 0$. It now remains to explain the problem of the curve form in the region $p < 10$. Since, as will be seen, the curvature of the curves always becomes smaller with diminishing p, both relatively to each other and also absolutely, it appears permissible to draw the κ curves as a first approximation between $p = 0$ and $p = 10$ as straight lines.

Figure 5 gives the function $N_{K=\infty}/N_K = f(p)$ in the range $0 < p < 10$ for different susceptibilities $[1.5 \leqq \kappa \leqq 10]$ on an enlarged scale. All the straight lines satisfy the simple relationship

$$\frac{N_{K=\infty}}{N_K} = c \cdot p + 1 \qquad \ldots\ldots (18)$$

---

* The approximation method will be briefly given here: We start from the equation of the straight line

$$y = f(x) = u + vx.$$

It is necessary so to determine u and v that

$$(y_1 - u - vx_1)^2 + (y_2 - u - vx_2)^2 + \ldots + (y_n - u - vx_n) = \text{minimum}$$

or briefly

$$\sum (y - u - vx)^2 = \text{minimum}.$$

Differentiation gives:

according to u: $\sum (y - u - vx) = 0$; according to v:

$$\sum x(y - u - vx) = 0,$$

or because here $\sum u = u \cdot n$,

$$\sum y - u \cdot n - v \sum x = 0 \text{ and } \sum xy - u \sum x - v \sum x^2 = 0.$$

From these equations we find:

$$u = \frac{\Sigma x \Sigma xy - \Sigma y \Sigma x^2}{(\Sigma x)^2 - n \Sigma x^2} \text{ and } v = \frac{\Sigma x \Sigma y - n \Sigma xy}{(\Sigma x)^2 - n \Sigma x^2}$$

In our case $u = 1$, so that only the constant v has to be calculated. For v we find the value $v = 0.0485$.

where C is a function of the susceptibility. The form of this function for $1 \leqq \kappa \leqq 10$ is shown by Figure 6. Equation (18) in combination with Figure 6 thus provides us with the following expressions for N for the present five cases of susceptibility:

$$\left.\begin{aligned} N_{\kappa = 1.5} &= \frac{N_{\kappa = \infty}}{0.028\, p + 1}\,, \\ N_{\kappa = 2} &= \frac{N_{\kappa = \infty}}{0.019\, p + 1}\,, \\ N_{\kappa = 3} &= \frac{N_{\kappa = \infty}}{0.012 + 1}\,, \\ N_{\kappa = 6} &= \frac{N_{\kappa = \infty}}{0.006 + 1}\,, \\ \text{and} \quad N_{\kappa = 10} &= \frac{N_{\kappa = \infty}}{0.0045\, p + 1} \end{aligned}\right\} \qquad \ldots\ldots (19)$$

Using equation (15) we have, if at the same time we write

$$\frac{1 + 2.35 \ln (1 + 0.137\, p)}{1 + 2.28 \ln (1 + 0.284\, p)} = Q \qquad \ldots\ldots (20)$$

$$\left.\begin{aligned} N_{\kappa = 1.5} &= \frac{N_{ell}}{0.28\, p + 1} \cdot Q \\ N_{\kappa = 2} &= \frac{N_{ell}}{0.019\, p + 1} \cdot Q \\ N_{\kappa = 3} &= \frac{N_{ell}}{0.012\, p + 1} \cdot Q \\ N_{\kappa = 6} &= \frac{N_{ell}}{0.006\, p + 1} \cdot Q \\ \text{and} \quad N_{\kappa = 10} &= \frac{N_{ell}}{0.0045\, p + 1} \cdot Q \end{aligned}\right\} \qquad \ldots\ldots (21)$$

where all the derivations apply only for $0 \leqq p \leqq 10$.

In the range $1 < \kappa \leqq 10$ and $0 \leqq p \leqq 10$ we obtain the following general expression to represent the demagnetisation factor

$$N_{1 < \kappa \leqq 10} = \frac{N_{ell}}{c \cdot p + 1} \cdot Q \qquad \ldots\ldots (22)$$

It is here assumed as axiomatic that the assumption of the rectilinear form of the function $N_{\kappa = \infty}/N_{\kappa} = f(p)$, made for the derivation of the equation system (19), may also be applied to κ values between $\kappa = 1$ and $\kappa = 1.5$, since, as was shown above, $N_{\kappa = \infty}/N_{\kappa = 1} = f(p)$ is likewise rectilinear.

If the solution of the equation system (21) is performed numerically for different p and κ values, we obtain the N or $N/4\pi$ values shown in Table 8.

5. $N_{0 < \kappa < 1}$ for $0 \leqq p \leqq 10$.

Since in the course of the subsequent investigations, it was found that the calculation of the demagnetisation factor in the range $0 < \kappa < 1$ by means of the above-mentioned approximation method was not successful, the demagnetisation factor $N_{0 < \kappa < 1}$ in the range $0 \leqq p \leqq 10$ was determined graphically. For this purpose, the curves for $\kappa = 0$ and $\kappa = 1$ known from equations (13) and (16) are also shown in Figure 4, in addition to the κ curves discussed above. If now in Figure 4 we draw a number of sections parallel to the abscissae axis, we obtain for $0 < \kappa < 1$ the curves shown in Figure 7, in which the susceptibility κ has been plotted as a function of p for different quotients $N_{\kappa = \infty}/N_{\kappa}$. This method of representation now enables us to determine the demagnetisation factors in a very simple way, as will be shown briefly with reference to two examples:

(a) We require the ballistic demagnetisation factor of a cylindrical bar of the dimension ratio $p = 8$ for the susceptibility $\kappa = 0.5$.

From Figure 7 we obtain for $p = 8$ and $\kappa = 0.5$ the value $N_{\kappa=\infty}/N_{\kappa=0.5} = 1.8$, i.e. $N_{\kappa=0.5} = N_{\kappa=\infty}/1.8$. From Table 4 or equation (15) the magnitude of $N_{\kappa=\infty}$ for the present case with $p = 8$ is found to be $N_{\kappa=\infty} = 0.26$, thus $N_{\kappa=1.5} = 0.26/1.8 = 0.15$.

(b) We require to know the value of $N_{\kappa=0.1}$ for the dimension ratio $p = 2$.

For the known values, Figure 7 gives us

$$\frac{N_{\kappa=\infty}}{N_{\kappa=0.1}} = 1.36 \quad \text{or} \quad N_{\kappa=0.1} = \frac{N_{\kappa=\infty}}{1.36} \; ;$$

with $N_{\kappa=\infty} = 1.70$ (according to Table 4 or equation (15)) we finally have

$$N_{\kappa=0.1} = 1.70/1.36 = 1.25 .$$

The application of this method to a number of p and κ values gives the demagnetisation factors shown in Table 9.

For $p > 10$, the graphical method is unnecessary, since in this case, the demagnetisation factors can be found from equation (4) of Stäblein and Schlechtweg.

IV. DISCUSSION OF THE RESULTS

In addition to a detailed discussion of the demagnetisation factors of cylindrical bars in the region $p < 10$, the present statements are intended to show the progress of the theoretical investigations carried out in Section III over the writer's previous calculations.

For this purpose, we first of all consider the two limit cases

$$N_{\kappa=0} \quad \text{and} \quad N_{\kappa=\infty}$$

The writer's previous considerations led to the following expressions for $N_{\kappa=0}$ and $N_{\kappa=\infty}$ on the basis of the approximation straight lines determined by the method of least squares:

$$N_{\kappa=0} = \frac{N_{ell}}{2.03 \cdot p^{0.319}} \; ; \qquad 1 \leq p \leq 100 \qquad \ldots\ldots (23)$$

and $$N_{\kappa=\infty} = 1.29 \cdot p^{0.383} \times N_{\kappa=0} \; ; \qquad 1 \leq p \leq 100 \qquad \ldots\ldots (24)$$

or represented as quotients:

$$\frac{N_{ell}}{N_{\kappa=0}} = 2.03 \, p^{0.319} \qquad \ldots\ldots (25)$$

and $$\frac{N_{\kappa=\infty}}{N_{\kappa=0}} = 1.29 \, p^{0.383} \; . \qquad \ldots\ldots (26)$$

Table 10 now compares the percentage deviations of the quotients $N_{ell}/N_{\kappa=0}$ and $N_{\kappa=\infty}/N_{\kappa=0}$ obtained by the earlier and present approximation methods from the ratio values calculated directly from equations (2), (3) and (6). The comparison shows that the new formulae, given here again

$$N_{\kappa=0} = \frac{N_{ell}}{2.28 \ln (1 + 0.284\, p) + 1} \; ; \quad 0 \leq p \leq 100 \quad \ldots\ldots (11)$$

and $$N_{\kappa=\infty} = N_{\kappa=0} \cdot [2.35 \ln (1 + 0.137\, p) + 1] \; ; \; 0 \leq p \leq 100 \quad \ldots\ldots (14)$$

with their small percentage deviations, i.e. higher relative accuracy are to be preferred to the expressions (23) and (24).

It should also be bo ne in mind that an increase in the ± deviation towards diminishing p values [for $p < 70$] no longer occurs in the new approximation method, which likewise allows one to conclude that there is a greater accuracy of the N values for $p < 10$. In addition to this advantage, there is a further improvement in the now possible calculation of the demagnetisation factors $N_{\kappa = 0}$ and $N_{\kappa = \infty}$ for the range $0 \leqq p \leqq 1$. The relationships (11) and (14) in addition to the same simple structure have also greater possibilities of practical application than the earlier equations (23) and (24).

With regard to the question of the absolute accuracy of the expressions derived, above all in the case $p < 10$, it is not possible at the moment to make a definite statement, since satisfactory experimental investigations of an extensive nature have not yet been made in this region [7] (see in this connection also Section V).

A further advantage resides in the extension of the problem to demagnetisation factors for susceptibilities $0 < \kappa < \infty$ and dimension ratios $0 \leqq p \leqq 10$. Attempts have already been made to express the demagnetisation factor in the shape of formulae on the basis of mathematical considerations. As was shown, it is possible to express the ballistic demagnetisation factors $N_{\kappa = 1}$ and $N_{1 < \kappa < 10}$ as a function of the dimension ratio p and the demagnetisation factor of ellipsoids, but it should be remembered that the accuracy of the $N_{1 < \kappa < 10}$ values is relatively less than that of the values $N_{\kappa = 0}$ and $N_{\kappa = 1}$ on account of the simplifications introduced in setting up the equations. The same applies to the graphically determined demagnetisation factors $N_{0 < \kappa < 1}$.

Figures 8a, 8b and 9 show the demagnetisation factor graphically as a function of the dimension ratio p or the susceptibility κ. In 8a and 8b, the demagnetisation factors of ellipsoids have also been plotted for comparison. With diminishing p, all the curves approach the limit value 4π. We see that in the region $p < 10$, the demagnetisation factors for susceptibilities $\kappa > 10$ are practically equivalent to the $N_{\kappa = \infty}$ values. For this reason the theoretical determination of N values for $\kappa > 10$ and $p < 10$ is unnecessary. The area bounded by the $N_{\kappa = 0}$ and $N_{\kappa = \infty}$ curves, therefore, for $p = 0$ to 10 is only filled by curve families of the susceptibilities $0 < \kappa < 10$. As follows from Figure 9, the demagnetisation factor diminishes with diminishing susceptibility for each dimension ratio p, this diminution being greater, the greater is p.

V. COMPARISON BETWEEN THEORY AND EXPERIMENT

A comparison will be made between theory and experiment on the basis of the paper by M.M. Tschetwerikowa [8]. This writer, by means of magnetisation curves, determined ballistically the demagnetisation factor of specimens of different shapes, including also cylindrical specimens of chromium, tungsten and cobalt steel with dimension ratios $0.3 \leqq p \leqq 25$. The real field was determined by measurements on a ring, made of the same material as the experimental bar. As is well known, this method of measurement is not entirely free from objection, since the properties of the ring and the bar may be quite different, being two quite different specimens. In this connection, the author of the paper points out that in her case any lack of homogeneity of the material could not greatly affect the results of the measurements, because the values she used in the calculations for the difference between the real and apparent field are sufficiently large in view of the small dimension ratios.

Of the numerous measurements, we shall deal here only with those made on chromium steel, since this material was considered by Tschetwerikowa as being the most homogeneous. The maximum susceptibility ($\kappa_{max} = [0.476 + 0.00568\, H_C] \cdot B_r / H_C$) [9] of the chromium steel is obtained from the indicated values of the remanence $B_r = 10,600$ and the coercive force $H_C = 47$ as κ_{max} = about 10. The experimental values of the demagnetisation factor in the range $0 < p < 10$ ought therefore to coincide with the theoretically found $N_{\kappa = \infty}$ values (cf. Table 4). Table 11 provides a comparison between the calculated $N_{\kappa = \infty}$ values and the demagnetisation factor obtained from the $N = f(p)$ curve of Tschetwerikowa*. Taking

---

* Tschetwerikowa's measurements extend to the region between κ_{max} and $\kappa = 0$ of the ascending branch of the magnetisation curve. According to the present author's investigations (Arch. Elektrotechn. 30 (1936) 761) the so-called hysteresis of the demagnetisation factor becomes smaller with decreasing κ_{max}. For the present case with $\kappa_{max} \approx 10$, it would be practically equal to zero, so that therefore the N values for the region above κ_{max} (of the ascending branch of the magnetisation curve) are identical with the N values below κ_{max}.

into consideration the accuracy of reading limited by the curve representation, the good agreement between theory and experiment is noteworthy*. The greater deviation occurring for $p = 1$ may perhaps be explained by the fact that the dimension ratio of the specimen was not determined with sufficient accuracy. As follows from Figure 8b, due to the steep rise of the $N = f(p)$ curves in the region $p < 10$, the dimension ratio p must be known all the more exactly the smaller p is, so as to keep N error as low as possible. Thus, for example, in the case $p = 1$, the N value varies by 18% for an error of the dimension ratio of only 2%.

The measurements of Thompson and Moss [10], who have also determined the ballistic demagnetisation factor of cylindrical bars with dimension ratios down to p = about 0.3 will not be discussed here in detail, since these authors wrongly defined the demagnetisation factor [11].

VI. THE IMPORTANCE OF THE BALLISTIC DEMAGNETISATION FACTOR OF CYLINDRICAL BARS FOR THE EVALUATION OF MAGNETIC MEASUREMENTS

The object of the following statements is to point out the need for a knowledge of accurate demagnetisation factors in practice, the errors occurring through the use of inexact demagnetisation factors and their influence on the evaluation of magnetic measurements being discussed in detail. In magnetic measurements in the free coil, the following equation is generally applicable**:

$$H = H' - NJ = H' - \frac{N}{4\pi}[B - H], \qquad \ldots\ldots (27)$$

where N is the demagnetisation factor, H' the coil field, H the field in the specimen, J the intensity of magnetisation and B the induction. The determination of the true field H in the specimen presents a well-known difficulty. If now the demagnetisation factor N is known, then if the external field H' is given, the true field H can be determined by shearing the $B - f(H')$ curve using the Rayleigh method [12].

For subsequent considerations, the true field H is not as interesting as the true permeability $\mu = B/H$. By division by B, equation (27) becomes [13]

$$\mu = \frac{1}{\frac{1}{\mu'} - \frac{N}{4\pi}\left[1 - \frac{1}{\mu}\right]}, \qquad \ldots\ldots (28)$$

or

$$\mu' = \frac{1}{\frac{1}{\mu} + \frac{N}{4\pi}\left[1 - \frac{1}{\mu}\right]}, \qquad \ldots\ldots (29)$$

where $\mu' = B/H'$ is the apparent permeability.

---

* The objection of improbability made in a previous article by the present author (Arch. Elektrotechn., 31 (1937) 124) against the whole of Tschetwerikowa's measurements on the basis of the theoretical results then available can no longer be maintained in view of the present calculations, which have been made with greater accuracy.

** Numerical equations are used in what follows. Cf. ETZ 51 (1930) 586; 53 (1932) 114 and Standard specification DIn 1313. The numerical values of H, H', J and B are referred to absolute electromagnetic units. As dimensional equation, expression (27) in accordance with the proposals of the Archiv f. Eletrotechnik will be

$$H = H' - \frac{1}{4\pi\mu_0} JN = H' - \frac{N}{4\pi}\left[\frac{B}{\mu_0} - H\right],$$

where μ_0 is the permeability of vacuum.

It will readily be seen from equation (28) that high accuracy in the calculation of the μ values is only to be expected if μ' and N are known with sufficient accuracy. In the converse case of the calculation of the apparent permeability from the true permeability [equation (29)], for high values of μ' the value of μ depends mainly upon N since there is a sum instead of a difference in the numerator of equation (29). The accuracy of μ' thus depends only upon the accuracy with which N is known.

These points of view which hold generally for the demagnetisation factor are applied in what follows to the special case of the ballistic demagnetisation factor of cylindrical bars.

With the aid of six graphical figures (10a to 10f) it will be shown for different dimension ratios D and a number of μ' values to what extent the magnitude of the true permeability is affected by an error in the determination of N.

The N error plotted as abscissae is here referred to the value obtained for $N_{K=\infty}$ according to the formulae (4) and (15). It will be seen from Figures 10a to 10f* that in the first place for a given dimension ratio D, an N error affects the permeability μ to a greater extent, the greater is μ'; secondly the curves show that the μ error diminishes with increasing dimension ratio D. From Table 12, which shows these relations numerically, it follows that in the determination of μ from μ' and N, even small percentage errors of the demagnetisation factor may alter the N value by 60% or more. Figure 11 shows the percentage μ error for constant N error of 20% plotted against μ' for different dimension ratios D. With decreasing μ', the curves approach the limit value $\mu' = 1$ for which the percentage μ error is equal to zero. It will be seen from the position of the curves that in particular for a large value of D, i.e. small N, the apparent permeability μ' must be known with greater accuracy, the smaller the inaccuracy of μ has to be.

If in Figure 11, for different μ errors, sections are drawn parallel to the abscissa axis, the curves shown in Figure 12 are obtained. These curves, on a double logarithmic scale, pass into parallel straight lines for D values greater than 30. The apparent permeability μ' has been plotted as ordinates. This mode of representation is generally of practical importance for magnetic measurements on cylinders inasmuch as it enables the necessary dimension ratio D for determining the true permeability μ to be read off if the errors of N and μ are given and the apparent permeability μ' is measured. For N errors $\gtrsim$ 20%, similar conditions obtain.

In amplification of what has been said, a paper by T. Nishina [14] will be discussed as practical example.

Nishina determined the permeability of a number of highly permeable materials by the ballistic method. The dimension ratio of his specimens was $D = 250$. The demagnetisation factor pertaining to this value was given by him on the basis of his own measurements as $N = 0.00075$ [15]. Table 13 shows Nishina's values for the initial and maximum permeability $[\mu_A]_I$ and $[\mu_{max}]_I$ as well as the μ'_A and μ'_{max} values of the unsheared curves calculated according to equation (29) with the demagnetisation factor $N = 0.00075$. The present author has shown elsewhere [16] that in the first place the ballistic demagnetisation factors determined by Nishina are always below the values for $N_{K=\infty}$ calculated from equation (4) according to Stäblein and Schlechtweg, and that secondly the difference between the calculated and experimentally determined N values always increases with increasing D. In the present case, with $D = 250$, the difference between the N values is almost 21% (N calculated = 0.000945, N measured = 0.00075).

If we regard the theoretically found value as the more correct - a reference to possible errors in Nishina's method of measurement is made in the footnote below** - the μ values obtained by him by shearing with too small a demagnetisation factor are thus really higher.

---

* These curves may also be applied to ellipsoids and cylindrical bars of a different susceptibility, it being merely necessary to remember that in this case, the demagnetisation factor must have a different dimension ratio.

** The considerable deviations of Nishina's measured values may be due in the first place to excessively long measuring coils (for the H-measurement) and also to the fact that the induction distribution depends considerably upon the cross-section variation and the material in the case of thin wires; the specimens had a diameter of 0.5 and 1 mm. Demagnetisation factors which are too small may also be due to the fact that the diameter of the coils used for the H-determination is too large compared with the diameter of the specimen [see in this connection E. Dussler: Ann. Phys., 86 (1928) 66]. It is not certain from Nishina's statements whether these conditions obtained in his case.

Table 13 shows the true permeabilities $[\mu_A]_{II}$ and $[\mu_{max}]_{II}$ for the demagnetisation factor $N_{\kappa=\infty} = 0.000945$, as calculated by means of equation (28) using the μ'_A and μ'_{max} values.

The last two columns of Table 13 contain the percentage differences (referred to the values provided with the index II) of μ_A and μ_{max}. It will clearly be seen that the N error, particularly for high μ' values is very appreciable - a variation of the true permeability of over 60% - whilst in the case of Super-Perminvar, with its low values of apparent permeability, the N error has no effect. This example clearly shows the importance of an accurate demagnetisation factor for the evaluation of magnetic measurements.

SUMMARY

1. The ballistic demagnetisation factors of cylindrical bars for the two limit susceptibilities $\kappa = 0$ and $\kappa = \infty$ and for dimension ratios $0 \leq p \leq 100$ using the demagnetisation factor of ellipsoids N_{ell} are calculated by means of an approximation method ensuring a greater accuracy compared with the author's earlier theoretical investigations.

2. The extension of the problem to the demagnetisation factors for susceptibilities $0 < \kappa < \infty$ and dimension ratios $p \geq 10$ led to the following results:

   (a) The ballistic demagnetisation factor of cylindrical bars for the susceptibility $\kappa = 1$ and dimension ratios $0 \leq p \leq 100$ may be represented in a simple form as a a function of the dimension ratio p and the demagnetisation factor of ellipsoids.

   (b) The ballistic demagnetisation factor for susceptibilities $1 < \kappa \leq 10$ and dimension ratios $0 \leq p \leq 10$ can be represented, as a first approximation, as a function of the dimension ratio and the demagnetisation factor of ellipsoids.

   (c) A graphical method is given for determining the ballistic demagnetisation factor for susceptibilities $0 < \kappa < 1$ and dimension ratios $p \leq 10$.

3. A comparison made for the case $\kappa = 10$ and $p = 10$ between calculated N values and demagnetisation factors determined experimentally by M.M. Tschetwerikowa gives good agreement.

4. The importance of ballistic demagnetisation factors of cylindrical bars for the evaluation of magnetic measurements is discussed with reference to a series of curves and to a practical example.

REFERENCES

[1] K. WARMUTH. Arch. Elektrotechn. 31 (1937) 124.

[2] E. DUSSLER. Ann. Phys., 86 (1928) 66.

[3] K. WARMUTH. Arch. Elektrotechn., 31 (1937) 124.

[4] F. STÄBLEIN and H. SCHLECHTWEG. Z. Phys. 95 (1935) 630.

[5] Further approximation formulae, especially for the limit case of infinitely large susceptibility will be found in: H. NEUMANN and K. WARMUTH. Wiss. Veröff. Siemens Konz., 11 (1932) 25 and K. WARMUTH. Arch. Elektrotechn. 31 (1937) 124.

[6] See in this connection J. WÜRSCHMIDT: Theorie des Entmagnetisierungfaktors. Brunswick. Vieweg and Sohn 1925. Also Du BOIS: Magnetische Kreise, p.43, Berlin. Julius Springer 1894.

[7] Regarding the experimental determination of the ballistic demagnetisation factor of cylindrical bars for $p > 10$ see inter alia K. WARMUTH. Arch. Elektrotechn. 30 (1936) 761. - J. WÜRSCHMIDT. Z. Phys. 19 (1923) 388. - S.P. BUDRIN. Journal of the Central Department for Weights and Measures (Russian paper), No. 4 (1930) 61. - E. DUSSLER. loc. cit.

[8] M.M. TSCHETWERIKOWA. Russ. Z. techn. Phys., 3 (1933) 1071.

[9] See in this connection ETZ 22 (1901) 696. Also E. GUMLICH. ETZ 44 (1923) 41.

[10] S.W. THOMPSON and E.W. MOSS. Proc. Phys. Soc., Lond., 21 (1909) 632.

[11] K. WARMUTH. Arch. Elektrotechn. 30 (1936) 761.

[12] Graetz. Handbuch der Elektrizität und des Magnetismus. pp.250 et seq. Leipzig, J.A. Barth. 1920.

[13] See in this connection MÜLLER-POUILLET. Lehrbuch der Physik und Meteorologie. Vol. 4, 1, p.92, 1909. W. STEINHAUS. Z. techn. Phys. 7 (1926) 495. H. NEUMANN. Wiss. Veröff. Siemens-Konz. X 2 (1931) 55; H. NEUMANN and K. WARMUTH. Wiss. Veröff. Siemens-Konz. XI (1932) 25.

[14] T. NISHINA. An investigation of some magnetic alloys. Rep. Tohoku Univ. 1936.

[15] T. NISHINA. On demagnetizing factor of cylindrical rods. Rep. Tohoku Univ. 24 (1935) No. 2.

[16] K. WARMUTH. Arch. Elektrotechn. 30 (1936) 761.

E.L.

TABLE 1

p	N_{ell} ACCORDING TO EQUATION (6)	$N_{K=0}$ ACCORDING TO EQUATION (2)	$\frac{N_{ell}}{N_{K=0}}$	$\frac{N_{ell}}{N_{K=0}}$ ACCORDING TO EQUATION (10)	± DEVIATION %
10	0.2549	0.0628	4.06	4.06	0.00
20	0.0847	0.0157	5.40	5.33	1.30
30	0.0433	0.000698	6.21	6.13	1.29
40	0.0266	0.00393	6.76	6.74	0.30
50	0.0181	0.00251	7.22	7.20	0.28
60	0.0132	0.00175	7.56	7.59	0.40
70	0.0101	0.00128	7.90	7.91	0.13
80	0.00801	0.000982	8.15	8.22	0.86
90	0.00651	0.000776	8.39	8.46	0.84
100	0.00541	0.000628	8.60	8.60	0.00
					Mean 0.54

TABLE 2

p	N_{ell} ACCORDING TO EQUATION (6)	$\frac{N_{ell}}{N_{K=0}}$ ACCORDING TO EQUATION (10)	$N_{K=0}$ ACCORDING TO EQUATION (11)	$\left[\frac{N}{4\pi}\right]_{K=0}$	p	N_{ell} ACCORDING TO EQUATION (7)	$\frac{N_{ell}}{N_{K=0}}$ ACCORDING TO EQUATION (10)	$N_{K=0}$ ACCORDING TO EQUATION (11)	$\left[\frac{N}{4\pi}\right]_{K=0}$
1	4.189	1.57	2.67	0.213	0.1	10.81	1.06	10.18	0.810
2	2.182	2.02	1.08	0.0860	0.2	9.43	1.13	8.36	0.666
3	1.366	2.40	0.570	0.0454	0.3	8.31	1.19	7.01	0.559
4	0.948	2.73	0.347	0.0276	0.4	7.39	1.25	5.94	0.473
5	0.702	3.01	0.233	0.0185	0.5	6.63	1.30	5.10	0.406
6	0.543	3.27	0.166	0.0132	0.6	5.98	1.36	4.41	0.352
7	0.435	3.49	0.125	0.00995	0.7	5.43	1.41	3.84	0.306
8	0.357	3.70	0.0966	0.00770	0.8	4.96	1.47	3.39	0.270
9	0.299	3.89	0.0770	0.00614	0.9	4.55	1.52	3.00	0.239
10	0.255	4.06	0.0628	0.00500	1.0	4.19	1.57	2.67	0.213

TABLE 3

p	$N_{K=\infty}$ ACCORDING TO EQUATION (3)	$N_{K=0}$ ACCORDING TO EQUATION (2)	$\frac{N_{K=\infty}}{N_{K=0}}$	$\frac{N_{K=\infty}}{N_{K=0}}$ ACCORDING TO EQUATION (13)	± DEVIATION %
10	0.190	0.0628	3.03	3.03	0.00
20	0.0651	0.0157	4.15	4.10	1.20
30	0.0342	0.00698	4.90	4.83	1.43
40	0.0214	0.00393	5.45	5.39	1.10
50	0.0148	0.00251	5.88	5.85	0.51
60	0.0109	0.00175	6.20	6.21	0.16
70	0.00840	0.00128	6.56	6.55	0.15
80	0.00670	0.000982	6.84	6.81	0.44
90	0.00546	0.000776	7.04	7.08	0.57
100	0.00460	0.000628	7.32	7.32	0.00
					Mean 0.46

TABLE 4

p	$\frac{N_{K=\infty}}{N_{K=0}}$ ACCORDING TO EQUATION (13)	$N_{K=\infty}$ ACCORDING TO EQUATION (15)	$\left[\frac{N}{4\pi}\right]_{K=\infty}$	p	$\frac{N_{K=\infty}}{N_{K=0}}$ ACCORDING TO EQUATION (13)	$N_{K=\infty}$ ACCORDING TO EQUATION (15)	$\left[\frac{N}{4\pi}\right]_{K=\infty}$
1	1.30	3.47	0.276	0.1	1.03	10.50	0.837
2	1.57	1.70	0.135	0.2	1.06	8.90	0.710
3	1.81	1.03	0.0820	0.3	1.09	7.66	0.611
4	2.02	0.704	0.0560	0.4	1.13	6.69	0.532
5	2.23	0.520	0.0415	0.5	1.16	5.90	0.470
6	2.41	0.400	0.0318	0.6	1.19	5.23	0.416
7	2.58	0.322	0.0256	0.7	1.22	4.66	0.372
8	2.74	0.264	0.0210	0.8	1.24	4.22	0.336
9	2.89	0.222	0.0177	0.9	1.27	3.82	0.304
10	3.03	0.190	0.0151	1.0	1.30	3.47	0.276

TABLE 5

p	$N_{K=\infty}$ ACCORDING TO EQUATION (3)	$N_{K=1}$ ACCORDING TO EQUATION (4) OR GRAPHICALLY DETERMINED*	$\frac{N_{K=\infty}}{N_{K=1}}$	$\frac{N_{K=\infty}}{N_{K=1}}$ ACCORDING TO EQUATION (16)	± DEVIATION %
10	0.190	0.130	1.46	1.49	2.02
20	0.0651	0.0338	1.93	1.97	2.03
30	0.0342	0.0137	2.50	2.46	1.63
50	0.0148	0.00411	3.60	3.43	4.95
80	0.00670	0.00137	4.88	4.88	0.00
100	0.00460	0.000800	5.75	5.85	1.71

* The mean deviation from the numerical values calculated strictly according to equation (4) is less than 3%.

TABLE 6

p	$\frac{N_{K=\infty}}{N_{K=1}}$ ACCORDING TO EQUATION (16)	$N_{K=1}$ ACCORDING TO EQUATION (17)	$\left[\frac{N}{4\pi}\right]_{K=1}$	p	$\frac{N_{K=\infty}}{N_{K=1}}$ ACCORDING TO EQUATION (16)	$N_{K=1}$ ACCORDING TO EQUATION (17)	$\left[\frac{N}{4\pi}\right]_{K=1}$
1	1.049	3.32	0.264	0.1	1.005	10.45	0.831
2	1.097	1.55	0.124	0.2	1.010	8.85	0.705
3	1.146	0.900	0.0716	0.3	1.015	7.55	0.601
4	1.194	0.590	0.0470	0.4	1.019	6.57	0.524
5	1.243	0.418	0.0333	0.5	1.024	5.76	0.460
6	1.291	0.310	0.0247	0.6	1.029	5.10	0.406
7	1.340	0.241	0.0192	0.7	1.034	4.51	0.359
8	1.388	0.190	0.0151	0.8	1.039	4.06	0.324
9	1.436	0.155	0.0123	0.9	1.044	3.66	0.292
10	1.485	0.128	0.0102	1.0	1.049	3.32	0.264

TABLE 7

p	N_K CALCULATED ACCORDING TO EQUATION (4) OR DETERMINED GRAPHICALLY					$\frac{N_{K=\infty}}{N_{K=1.5}}$	$\frac{N_{K=\infty}}{N_{K=2}}$	$\frac{N_{K=\infty}}{N_{K=3}}$	$\frac{N_{K=\infty}}{N_{K=6}}$	$\frac{N_{K=\infty}}{N_{K=10}}$
	$N_{K=1.5}$	$N_{K=2}$	$N_{K=3}$	$N_{K=6}$	$N_{K=10}$					
10	0.149	0.160	0.170	0.179	0.182	1.28	1.19	1.12	1.06	1.045
20	0.0413	0.0470	0.0525	0.0566	0.593	1.58	1.39	1.24	1.15	1.10
30	0.0177	0.0206	0.0239	0.0268	0.0288	1.93	1.66	1.43	1.28	1.19
40	0.00930	0.0109	0.0130	0.0148	0.0162	2.30	1.96	1.65	1.45	1.32
50	-	0.00650	0.00780	0.00910	0.0100	-	2.28	1.90	1.63	1.47

TABLE 8

p	$\frac{N_{K=\infty}}{N_{K=1.5}}$ ACCORDING TO FIG.5	$N_{K=1.5}$ ACCORDING TO EQUATION (21)	$\left[\frac{N}{4\pi}\right]_{K=1.5}$	$\frac{N_{K=\infty}}{N_{K=3}}$ ACCORDING TO FIG.5	$N_{K=3}$ ACCORDING TO EQUATION (21)	$\left[\frac{N}{4\pi}\right]_{K=3}$	$\frac{N_{K=\infty}}{N_{K=10}}$ ACCORDING TO FIG. 5	$N_{K=10}$ ACCORDING TO EQUATION (21)	$\left[\frac{N}{4\pi}\right]_{K=10}$
1	1.028	3.380	0.269	1.013	3.425	0.273	1.005	3.450	0.275
2	1.056	1.610	0.128	1.025	1.660	0.132	1.008	1.690	0.135
4	1.113	0.630	0.0502	1.048	0.672	0.0535	1.018	0.693	0.0552
6	1.168	0.343	0.0273	1.073	0.373	0.0297	1.025	0.391	0.0311
8	1.225	0.216	0.0172	1.095	0.241	0.0192	1.035	0.256	0.0204
10	1.280	0.149	0.0119	1.120	0.170	0.0135	1.045	0.182	0.0145

TABLE 9

p	$N_{K=0.1}$	$\left[\frac{N}{4\pi}\right]_{K=0.1}$	$N_{K=0.3}$	$\left[\frac{N}{4\pi}\right]_{K=0.3}$	$N_{K=0.5}$	$\left[\frac{N}{4\pi}\right]_{K=0.5}$	$N_{K=0.7}$	$\left[\frac{N}{4\pi}\right]_{K=0.7}$
1	3.05	0.243	3.10	0.247	3.16	0.252	3.30	0.262
2	1.25	0.0995	1.34	0.107	1.45	0.115	1.51	0.120
4	0.39	0.0310	0.45	0.0358	0.50	0.0398	0.55	0.0438
6	0.19	0.0151	0.22	0.0175	0.25	0.0199	0.28	0.0223
8	0.10	0.00795	0.13	0.0104	0.15	0.0119	0.17	0.0135
10	0.064	0.00510	0.080	0.00636	0.095	0.00756	0.11	0.00875

TABLE 10

p	± DEVIATION FOR $\frac{N_{all}}{N_{K=0}}$		± DEVIATION FOR $\frac{N_{K=\infty}}{N_{K=0}}$	
	OLD METHOD [Eq. (25)]	NEW METHOD [Eq. (10)]	OLD METHOD [Eq. (26)]	NEW METHOD [Eq. (13)]
10	4.67	0.00	2.97	0.00
20	2.04	1.30	2.17	1.20
30	3.06	1.29	3.45	1.43
40	2.52	0.30	3.46	1.10
50	1.94	0.28	1.70	0.51
60	0.66	0.40	0.00	0.16
70	0.25	0.13	0.15	0.15
80	1.10	0.86	1.03	0.44
90	1.79	0.84	2.56	0.57
100	2.90	0.00	2.73	0.00

TABLE 11

p	$N_{\kappa=\infty}$ ACCORDING TO EQ. (15)	N FOR CHROMIUM STEEL ACCORDING TO M.M. TSCHETWERIKOWA	DEVIATION (REFERRED TO CALCULATED VALUE) IN ROUND FIGURES %
1	3.47	2.90	- 16
2	1.70	1.65	- 3
3	1.03	1.05	+ 2
4	0.70	0.72	+ 3
5	0.52	0.51	- 2
6	0.40	0.38	- 5
7	0.32	0.31	- 3
8	0.26	0.25	- 4
9	0.22	0.22	0
10	0.19	0.19	0

TABLE 12

N ERROR %	μ ERROR %																					
	$\mu' = 10$						$\mu' = 100$						$\mu' = 1000$						$\mu' = 10000$			
	$p =$						$p =$						$p =$						$p =$			
	5	10	50	100	250	500	5	10	50	100	250	500	5	10	50	100	250	500	5	10	50	100	250	500
5	3.5	1					μ		0.5	0.3	μ		μ ERROR			3.5	0.5	μ ERROR LESS THAN 1%					10	1.5
10	6.5	1.5	μ ERROR LESS				ERROR		1	0.5	ERROR		GREATER			6	1		μ ERROR GREATER				19	3
30	16	4.5	THAN 1%				GREATER		3	1	LESS		THAN			16	8		THAN 60%				44	18
50	25	7.5					THAN		5	2	THAN		60%			24	4						58	12
							60%				1%													

TABLE 13

MATERIAL	PERMEABILITY ACCORDING TO NISHINA WITH $N = 0.00075$		APPARENT PERMEABILITY CALCULATED ACCORDING TO EQ. (29) WITH $N = 0.00075$		PERMEABILITY CALCULATED ACCORDING TO EQ. (28) WITH $N = 0.000945$		DEVIATION %	
							$\frac{(\mu_A)_{II}-(\mu_A)_I}{(\mu_A)_{II}} \cdot 100$	$\frac{(\mu_{max})_{II}-(\mu_{max})_I}{(\mu_{max})_{II}} 100$
	$(\mu_A)_I$	$(\mu_{max})_I$	μ'_A	μ'_{max}	$(\mu_A)_{II}$	$(\mu_{max})_{II}$		
Super-Permalloy 1	13000	44000	7300	12100	16100	131500	19.3	66.5
Super-Permalloy 2	12800	40000	7250	11800	15900	100000	19.5	60
Super-Permalloy 3	15700	39500	8100	11700	20600	95400	23.8	58.5
Super-Perminvar	63.5	560	63.3	540	63.8	565	0.5	0.9

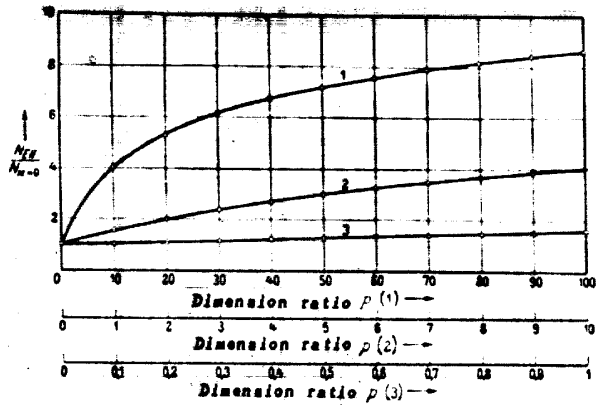

Fig. 1: The quotient $N_{ell}/N_{K=0}$ plotted against the dimension ratio p.

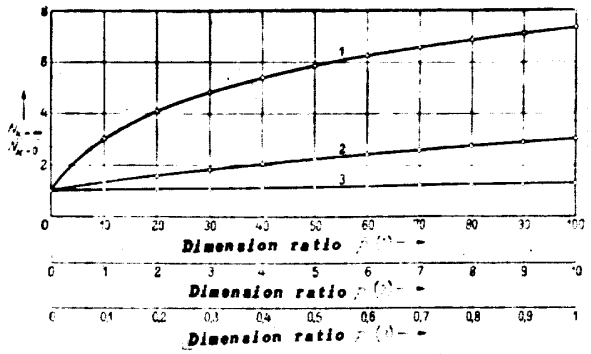

Fig. 2: The quotient $N_{K=\infty}/N_{K=0}$ plotted against the dimension ratio p.

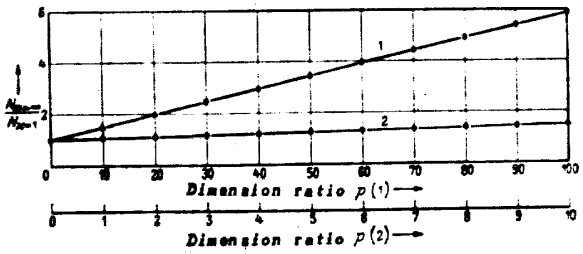

Fig. 3: The quotient $N_{K=\infty}/N_{K=1}$ as a function of the dimension ratio p.

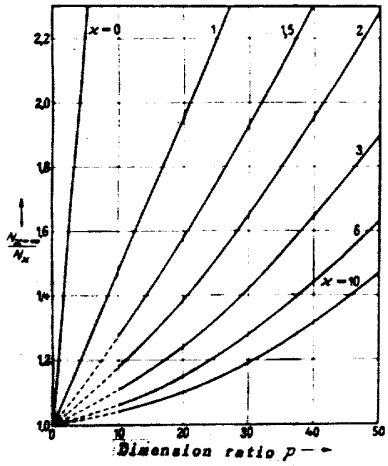

Fig. 4: The quotient $N_{K=\infty}/N_{K}$ as a function of the dimension ratio p for different susceptibilities K as parameter.

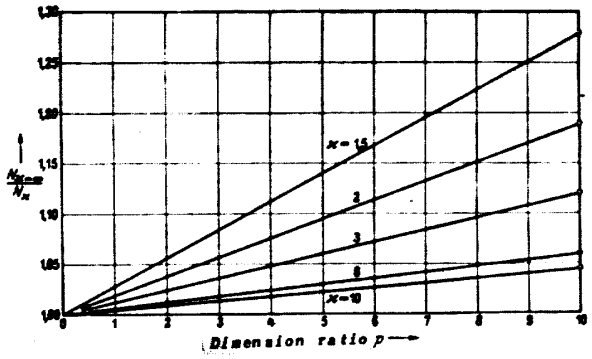

Fig. 5: $N_{K=\infty}/N_{K}$ as a function of the dimension ratio p for different susceptibilities K as parameter.

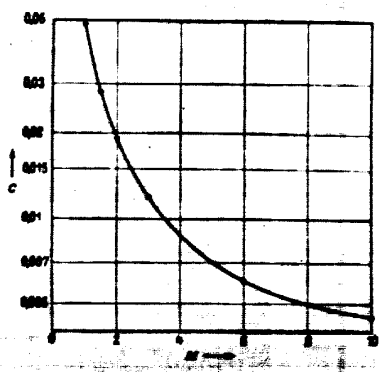

Fig.6: The magnitude c plotted as a function of the susceptibility κ.

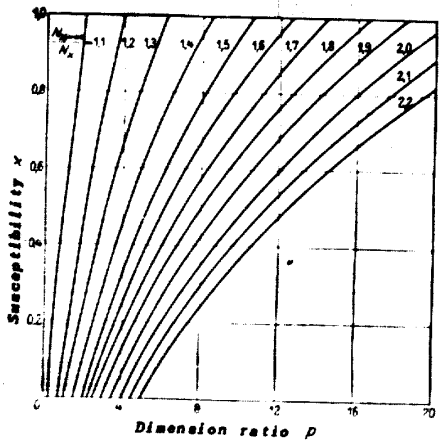

Fig.7: Susceptibility κ as a function of the dimension ratio for different $N_\kappa = \omega/N_\kappa$ values as parameter.

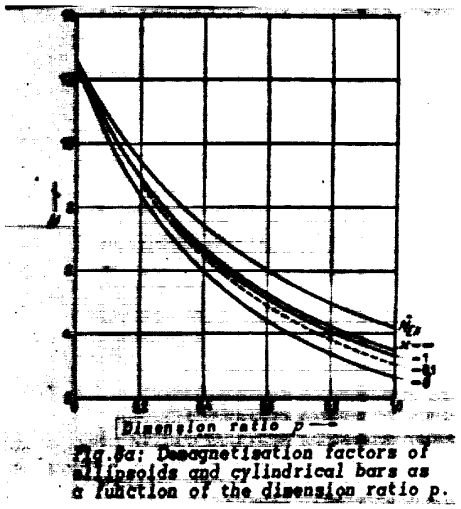

Fig.8a: Demagnetisation factors of ellipsoids and cylindrical bars as a function of the dimension ratio p.

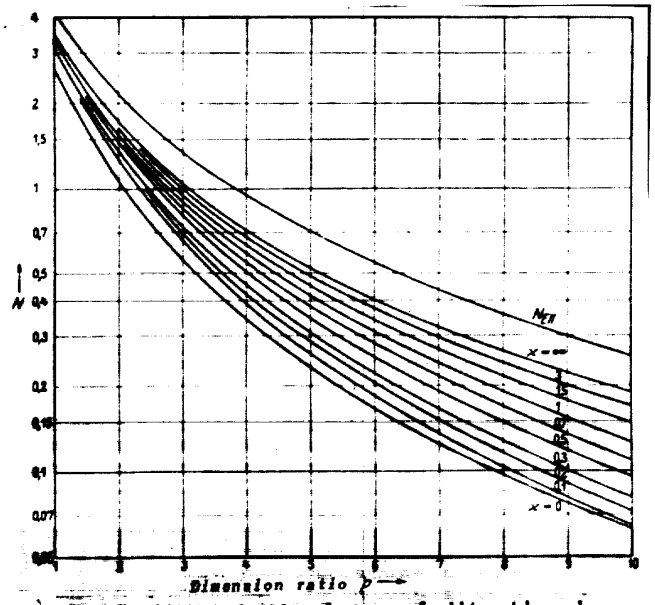

Fig.8b: Demagnetisation factors of ellipsoids and cylindrical bars as a function of the dimension ratio p.

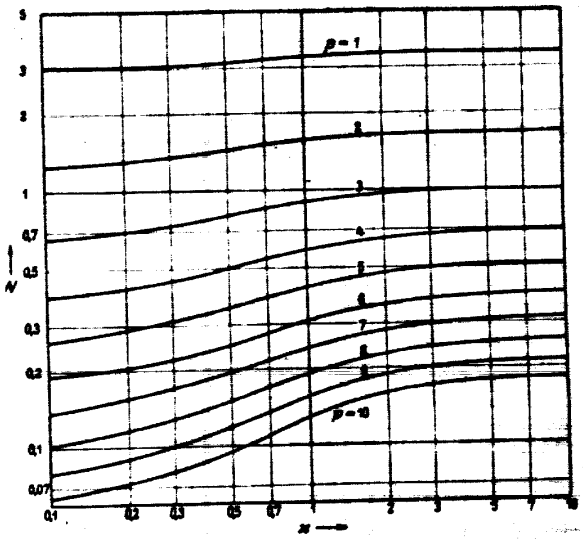

Fig.9: Demagnetisation factor N plotted against susceptibility κ for dimension ratios p = 1 to 10.

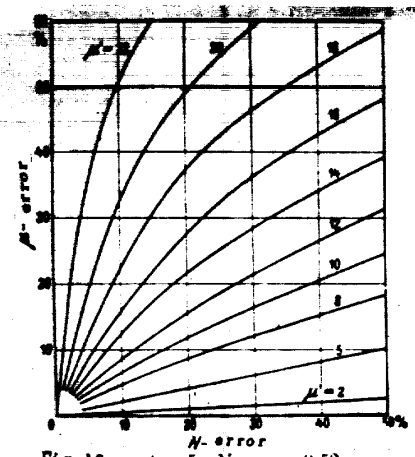

Fig.10a: $p = 5$; $N_{x=\infty} = 0{,}52$.

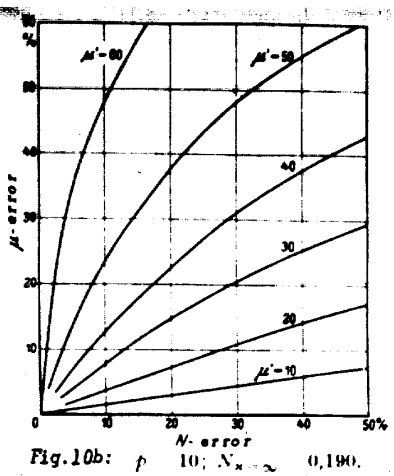

Fig.10b: $p = 10$; $N_{x=\infty} = 0{,}190$.

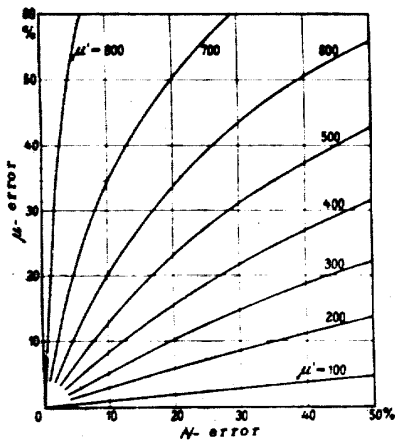

Fig.10c: $p = 50$; $N_{x=\infty} = 0{,}0151$.

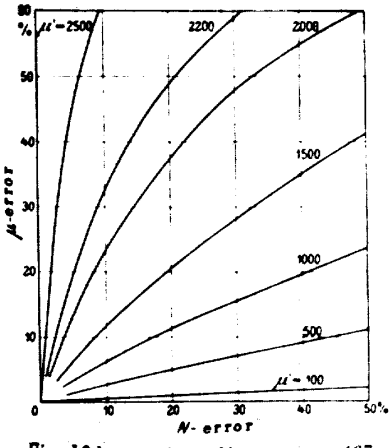

Fig.10d: $p = 100$; $N_{x=\infty} = 0{,}00467$.

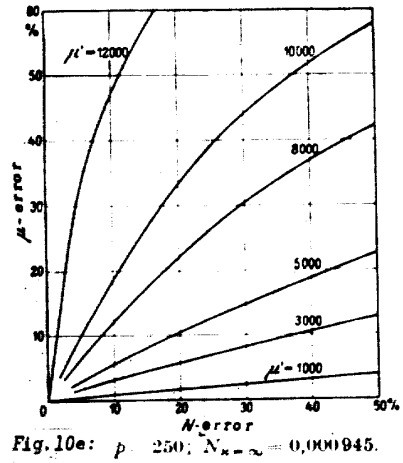

Fig.10e: $p = 250$; $N_{x=\infty} = 0{,}000945$.

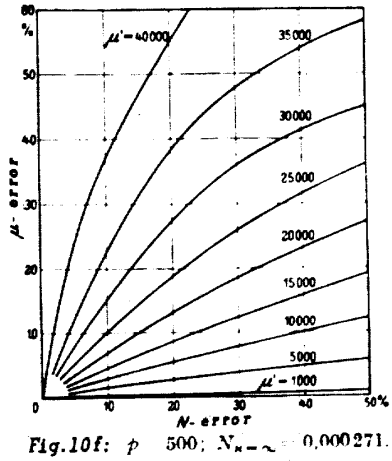

Fig.10f: $p = 500$; $N_{x=\infty} = 0{,}000271$.

Figs. 10a to f: Percentage μ error as a function of the percentage N errors for different apparent permeabilities μ' and dimension ratios p.

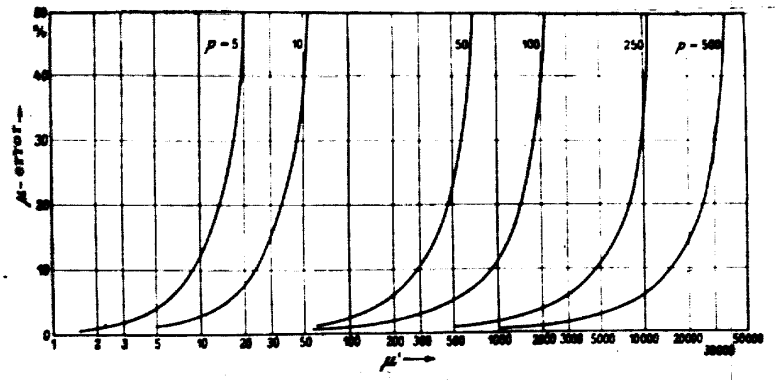

Fig.11: Percentage μ error as a function of the apparent permeability μ' for different p values as parameter with a constant N error of 20%.

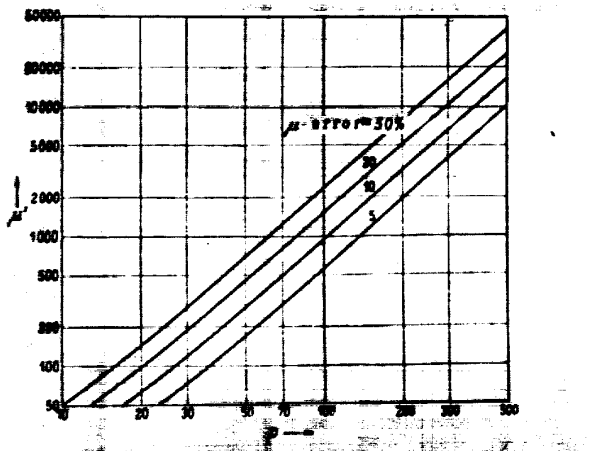

Fig.12: Apparent permeability μ' as a function of the dimension ratio p for different percentage μ errors as parameter with a constant N error of 20%.